# Detailed discussion of a linear electric field frequency shift induced in confined gases by a magnetic field gradient: Implications for neutron electric-dipole-moment experiments

S. K. Lamoreaux[1] and R. Golub[2,*]

[1]*University of California, Los Alamos National Laboratory, Physics Division, Los Alamos, New Mexico 87545, USA*
[2]*Physics Department, North Carolina State University, Raleigh, North Carolina 27606, USA*
(Received 17 September 2004; published 14 March 2005)

The search for particle electric dipole moments (EDM's) is one of the best places to look for physics beyond the standard model of electroweak interaction because the size of time reversal violation predicted by the standard model is incompatible with present ideas concerning the creation of the baryon-antibaryon asymmetry. As the sensitivity of these EDM searches increases more subtle systematic effects become important. We develop a general analytical approach to describe a systematic effect recently observed in an electric dipole moment experiment using stored particles [J. M. Pendlebury *et al.*, Phys. Rev. A **70**, 032102 (2004)]. Our approach is based on the relationship between the systematic frequency shift and the velocity autocorrelation function of the resonating particles. Our results, when applied to well-known limiting forms of the correlation function, are in good agreement with both the limiting cases studied in recent work that employed a numerical and heuristic analysis. Our general approach explains some of the surprising results observed in that work and displays the rich behavior of the shift for intermediate frequencies, which has not been studied previously.

## I. INTRODUCTION

The search for an electric dipole moment (EDM) of the neutron is perhaps unique in modern physics in that experimental work on this subject has been going on more or less continuously for over 50 years. In that period the experimental sensitivity has increased by more than a factor of $10^6$ without an EDM ever being observed. The reason for this apparently obsessive behavior by a small group of dedicated physicists is that the observation of a nonzero neutron EDM would be evidence of time reversal violation and for physics beyond the so-called standard model of electroweak interactions. An essential point is that the standard model predictions of the magnitude of time reversal violation are inconsistent with our ideas of the formation of the universe; namely, the production of the presently observed matter-antimatter asymmetry requires time reversal violation many orders of magnitude greater than that predicted by the standard model.

In this type of experiment (null experiment) the control of systematic errors is of great significance. While the switch of experimental technique from beam experiments to experiments using stored ultracold neutrons (UCN's) has eliminated many of the sources of systematic error associated with the beam technique, the gain in sensitivity brought by the new UCN technique means that the experiments are sensitive to a new range of systematic errors. One of the most serious of these is associated with the interaction of gradients of the ever-present constant magnetic field with the well-known motional magnetic field ($\vec{E} \times \vec{v}/c$). As the particles move in the apparatus, these fields, as seen by the particles, will be time dependent. This effect was first pointed out by Commins [1] and explained in terms of the geometrical phase

concept. A more general description is in terms of the Bloch-Siegert (BS) shift of magnetic resonance frequencies due to the time-dependent fields mentioned above [2,3].

The effect was apparently empirically identified in the ILL Hg comagnetometer EDM experiment, and recently Pendlebury *et al.* [2] have given a very detailed discussion of it, including intuitive models and analytical calculations for certain cases, the relation between and regions of applicability of the geometric phase and Bloch-Siegert models, numerical simulations, and experimental verification of the most significant features. However, this pioneering work has left certain questions unanswered. In particular the understanding of the effects of collisions on the systematic frequency shifts remain incomplete.

In this work we attempt to clarify several points concerning the influence of particle collisions. We explain the reason that in contrast to gas collisions, collisions with the walls were observed to have no effect on the magnitude of the systematic frequency shifts and show that this only applies to the limiting cases of high and low frequencies. We show that the frequency shift is related to the velocity autocorrelation function of the resonating particles. Our solution, when applied to well-known limiting forms of the correlation function, gives results in agreement with those obtained numerically in [2]. McGregor has taken a similar approach to the problem of relaxation due to static field gradients [4], whereas the approach taken by Cates *et al.* to the problem of static field gradients [5] and gradients combined with oscillating perturbing fields [6] is somewhat different than ours.

### Brief description of the effect

Consider a case where, in a storage experiment, there is a radial magnetic field due to a magnetic field gradient in the $z$ direction ($B_0$, the quantization axis, and the electric field $E$ are along $z$). Now consider roughly circular orbits, due to

*Present address: Hahn Meitner Institut, Berlin, Germany.

specular reflection around the bottle at a constant angle, in the $x$-$y$ plane with radius approximately the bottle radius $R$. The wall collisions occur at a frequency $1/\tau_c$ while the orbital frequency is $\omega_r = 2\alpha/\tau_c$ where $\alpha$ is the incidence angle relative to the surface. We can transform into a rotating frame at $\omega_r$ (note that this is not the Schwinger rotating frame that eliminates $B_0$) so that the problem is quasistatic [3].

The radial field, with the barrel gradient plus $E \times v$ field, is

$$B_R = B_r \pm B_E = aR \pm \frac{\omega_r RE}{c},$$

where $B_r(r) = (r/2)\partial B_z/\partial z = ar$ is the radial field due to the axial gradient, $\pm B_E = r\omega_r E/c$ is the radially directed $E \times v$ field, and the $\pm$ refer to the rotation direction.

In the rotating frame,

$$B^2 = (B_0 - \omega_r/\gamma)^2 + (B_R)^2,$$

where $\gamma$ is the gyromagnetic ratio. Expanding in the limit where $B_R \ll B_0$ with transformation back to the laboratory frame we find

$$B = B_0 + \frac{1}{2}\frac{(aR - \omega_r RE/c)^2}{B_0 - \omega_r/\gamma} = B_0 - \frac{(aR^2\omega_r E/c)}{B_0 - \omega_r/\gamma},$$

keeping only terms linear in $B_E$. Averaging over the rotation direction (e.g., the sign of $\omega_r$), the net effect of the gradient field combined with an $E \times v$ yields a systematic (magnetic field) shift of

$$\delta\omega = \gamma\delta B = -\frac{\gamma^2 av^2 E}{c(\omega_0^2 - \omega_r^2)}, \tag{1}$$

equivalent to Eq. (18) of [2]. Taking the limit $\omega_r/\gamma \ll B_0$ we have

$$\delta B = -\frac{aR^2\omega_r^2 E}{\gamma cB_0^2}, \quad \delta\omega = -\frac{aR^2\omega_r^2 E}{cB_0^2}, \tag{2}$$

which would seem to set the scale of the effect and is equivalent to Eq. (19) of [2]. In this limit, the frequency shift does not depend on $\gamma$, implying that it is the result of a geometric effect.

In the other limit, where the rotation frequency is much faster than the Larmor frequency, we similarly find that

$$\delta B = \gamma aR^2 E/c, \quad \delta\omega = \gamma^2 aR^2 E/c, \tag{3}$$

which is independent of the motional frequency $\omega_r$, of opposite sign from the previous limit, and equivalent to Eq. (21) of [2].

## II. FREQUENCY SHIFT DUE TO FLUCTUATING FIELDS IN THE $x$-$y$ PLANE

### A. Density matrix approach to the problem

The issues of the effects of a weak fluctuating potential on the evolution of the density matrix have been well addressed in the literature. However, these treatments generally assume

that the perturbing potential has a short correlation time, and certain assumptions regarding averaging are not applicable to our problem. The effect of a static electric field $E$ by itself was treated in [7] where the $E^2$ effect was related to the correlation time and requirements on the field reversal accuracy were discussed.

So we therefore start from the beginning, following [8] (p. 276).

The radial gradient and $E \times v$ fields can be treated as weak fluctuating perturbing fields $B_{x,y}(t)$ in the $x$-$y$ plane, with a constant $B_0$ applied along $z$. The perturbing fields $B'_{x,y}(t)$ can be written as

$$B'_x(t) = B_x(t) - \langle B_x(t)\rangle, \quad B'_y(t) = B_y(t) - \langle B_y(t)\rangle, \tag{4}$$

where $\langle\cdots\rangle$ represents a time average of $B_{x,y}(t)$. The constant components of the perturbing field are added to $B_0$,

$$B'_0 = \sqrt{(B_0)^2 + \langle B_x(t)\rangle^2 + \langle B_y(t)\rangle^2}, \tag{5}$$

leaving the perturbing fields with averages of zero. We define

$$\omega_0 = \gamma B'_0, \quad \omega_{x,y}(t) = \gamma B'_{x,y}(t). \tag{6}$$

The Hamiltonian is thus

$$H = -\frac{\omega_0}{2}\sigma_z - \frac{\omega_x}{2}\sigma_x - \frac{\omega_y}{2}\sigma_y = H_0 + H_1(t). \tag{7}$$

Defining

$$2b = \omega_x + i\omega_y, \quad 2b^* = \omega_x - i\omega_y, \tag{8}$$

the perturbing Hamiltonian can be rewritten as

$$H_1(t) = b^*\sigma_+ + b\sigma_-, \tag{9}$$

where $\sigma_\pm$ are defined in the Appendix, and it is understood that $b$ is intrinsically time dependent. Furthermore, the density matrix can be expanded in the spherical Pauli basis,

$$\rho = 1 + \rho_{1,0}\sigma_z + \rho_{1,1}\sigma_+ + \rho_{1,-1}\sigma_-, \tag{10}$$

where $\rho_{11} = \rho_{1-1}^*$.

The time evolution of the density matrix is

$$\frac{d\rho}{dt} = -i[H_0 + H_1(t), \rho]. \tag{11}$$

The explicit dependence on the constant $H_0$ can be eliminated by transforming to the rotating frame (also called the interaction representation), with

$$H_1(t) \rightarrow e^{iH_0 t}H_1(t)e^{-iH_0 t}, \quad \rho \rightarrow e^{iH_0 t}\rho e^{-iH_0 t}, \tag{12}$$

where

$$e^{iH_0 t} = \begin{pmatrix} e^{-i\omega_0 t/2} & 0 \\ 0 & e^{i\omega_0 t/2} \end{pmatrix}. \tag{13}$$

We henceforth will work in the rotating frame, with

$$H_1(t) = e^{-i\omega_0 t}b^*\sigma_+ + e^{i\omega_0 t}\sigma_-. \tag{14}$$

The time evolution of the density matrix in the rotating frame is

$$\frac{d\rho}{dt} = -i[H_1(t), \rho], \qquad (15)$$

which can be integrated by successive approximations to

$$\rho(t) = \rho(0) - i \int_0^t [H_1(t'), \rho(0)]dt'$$

$$- \int_0^t dt' \int_0^{t'} dt'' [H_1(t'), [H_1(t''), \rho(0)]]. \qquad (16)$$

We are interested in the relaxation rates and frequency shifts due to the perturbing fields, which can be found through the time derivative of $\rho$, which, by introducing a new variable $\tau = t - t''$, is

$$\frac{d\rho}{dt} = -i[H_1(t), \rho(0)] - \int_0^t d\tau [H_1(t), [H_1(t - \tau), \rho(0)]]. \qquad (17)$$

The first term on the right-hand side (RHS) has an ensemble average of zero; furthermore, there is no correlation between $\rho$ and the fluctuating Hamiltonian [e.g., phases of the neutrons have no explicit spatial dependence and $H_1(t)$ is different for every neutron in the system]. In addition, if we assume that the perturbation is weak, $\rho(0)$ can be replaced by $\rho(t)$ which introduces errors below second order.

We then have

$$\frac{d\rho}{dt} = -\int_0^t d\tau [H_1(t), [H_1(t - \tau), \rho(t)]] \equiv \Gamma \rho(t), \qquad (18)$$

where $\Gamma$ is the "relaxation matrix," the real parts of which describe decays of coherence and the imaginary parts of the off-diagonal elements describe frequency shifts.

Using the relations in the Appendix together with the expansion of the density matrix, Eq. (10), the time derivative of $\rho$, correct to second order and neglecting $2\omega_0$ terms, is

$$\dot{\rho}_{1,-1} = -\rho_{1,-1} \int_0^t 2e^{i\omega_0 \tau} b^* b' d\tau, \qquad (19)$$

$$\dot{\rho}_{1,1} = -\rho_{1,1} \int_0^t 2e^{-i\omega_0 \tau} b b'^* d\tau, \qquad (20)$$

$$\dot{\rho}_{1,0} = -\rho_{1,0} \int_0^t 4 \, \mathrm{Re}[e^{i\omega_0 t} b'^* b] d\tau, \qquad (21)$$

where

$$2b = \omega_x(t) + i\omega_y(t), \quad 2b' = \omega_x(t - \tau) + i\omega_y(t - \tau). \qquad (22)$$

These equations describe both a frequency shift and relaxation rates of the density matrix. We are at present most interested in the frequency shift, which is given by the difference in the off-diagonal components of $\Gamma$. Expanding $b$ and $b'$ we find

$$\delta\omega(t) = -\frac{1}{2} \int_0^t \{\cos \omega_0 \tau [\omega_x(t)\omega_y(t - \tau) - \omega_x(t - \tau)\omega_y(t)]$$

$$+ \sin \omega_0 \tau [\omega_x(t)\omega_x(t - \tau) + \omega_y(t)\omega_y(t - \tau)]\}d\tau. \qquad (23)$$

This is the general solution for the frequency shift given an arbitrary perturbing field. An ensemble average must be taken.

The identical result is obtained with appropriate $(\omega_{x,y}, \delta\omega \ll \omega_0)$ approximations from the Bloch equation in the form given in Eqs. (46) and (47) of [2]. This is quite interesting given the different assumptions made in the two approaches.

Now $\omega_x = ax + bv_y$, $\omega_y = ay - bv_x$ where

$$a = \frac{\gamma}{2} \frac{\partial B_z}{\partial z}, \qquad (24)$$

$$b = \gamma \frac{E}{c}, \qquad (25)$$

with $\gamma$ the gyromagnetic ratio, and it is clear that only the cross terms $\omega_x \omega_y$ will result in a nonzero linear $E(\propto b)$ shift,

$$\delta\omega = -\frac{1}{2} \int_0^t d\tau (\cos \omega_0 \tau) \{\langle \omega_x(t)\omega_y(t - \tau)\rangle - \langle \omega_x(t - \tau)\omega_y(t)\rangle\}$$

$$= \frac{ab}{2} \int_0^t d\tau (\cos \omega_0 \tau) R(\tau), \qquad (26)$$

where

$$R(\tau) = \langle y(t)v_y(t - \tau) + x(t)v_x(t - \tau) - y(t - \tau)v_y(t)$$

$$- x(t - \tau)v_x(t)\rangle \qquad (27)$$

is the net correlation function, where $\langle \cdots \rangle$ represents an ensemble and time average.

### B. General solution for a radial magnetic field plus $E \times v$ field

According to Eq. (26) the frequency shift is proportional to the cosine Fourier transform of the correlation function $R(\tau)$, between $(y, v_y)$ and $(x, v_x)$ evaluated at the Larmor frequency $\omega_0$. However, this can be written in terms of the velocity autocorrelation function as follows:

$$y(t) = y_0 + \int_0^t v_y(t')dt',$$

$$y(t - \tau) = y_0 + \int_0^{t - \tau} v_y(t')dt'. \qquad (28)$$

Since there are no correlations between $y_0$ and $v_y$, the $y$ terms in Eq. (27) are

$$A = y(t)v_y(t - \tau) = \int_0^t \langle v_y(t')v_y(t - \tau)\rangle dt', \qquad (29)$$

$$B = y(t - \tau)v_y(t) = \int_0^{t-\tau} \langle v_y(t')v_y(t) \rangle dt', \qquad (30)$$

$$R_y(\tau) = A - B = \left( \int_0^t \langle v_y(t')v_y(t - \tau) \rangle dt' \right.$$
$$\left. - \int_0^{t-\tau} \langle v_y(t')v_y(t) \rangle dt' \right) \qquad (31)$$

$$= \int_{\tau-t}^\tau dx \psi(x) - \int_\tau^t dx \psi(x), \qquad (32)$$

where $\psi(x)$ is the velocity autocorrelation function and we used the fact that it is an even function of $x$. Repeating the same argument for the $x$ axis we have

$$\psi(\tau) = \langle v_y(t)v_y(t - \tau) + v_x(t)v_x(t - \tau) \rangle = \langle \vec{v}_{xy}(t) \cdot \vec{v}_{xy}(t - \tau) \rangle,$$

$$R(\tau) = \int_{\tau-t}^\tau dx \psi(x) - \int_\tau^t dx \psi(x) \qquad (33)$$

$$= 2h(\tau) - h(t - \tau) - h(t) \qquad (34)$$

$$= 2h(\tau), \qquad (35)$$

$$h(\tau) = \int_0^\tau dx \psi(x), \qquad (36)$$

and we consider only cases where $\psi(x) \to 0$ as $x \to \infty$ so that we can take the limit $t \to \infty$ in Eq. (34) and we note that a constant term in $R$ will not have any effect on Eq. (26), contributing only a term $\propto \delta(\omega_0) = 0$.

According to Eq. (26) we need the cosine Fourier transform (FT) of $R(\tau)$. This will involve $1/\omega$ times the FT of $\psi(x)$ which in turn is proportional to $\omega^2$ times the FT of the position correlation function as we shall see. Substituting Eq. (35) into Eq. (26) we have

$$\delta\omega = ab \int_0^t d\tau (\cos \omega_0 \tau) h(\tau). \qquad (37)$$

Writing the velocity correlation function as

$$\psi(t) = \int_{-\infty}^\infty \cos \omega t \psi(\omega) d\omega, \qquad (38)$$

we have

$$h(\tau) = \int_0^\tau \psi(t) dt = \int_{-\infty}^\infty \psi(\omega) \left( \frac{\sin \omega\tau - 1}{\omega} \right) d\omega, \qquad (39)$$

so that according to Eq. (37) the frequency shift is given by (dropping the time-independent term)

$$\delta\omega = ab \left[ \int_0^t d\tau \cos \omega_0 \tau \int_{-\infty}^\infty \psi(\omega) \frac{\sin \omega\tau}{\omega} d\omega \right],$$

$$\delta\omega = -ab \int_{-\infty}^\infty \frac{\psi(\omega)}{(\omega_0^2 - \omega^2)} d\omega. \qquad (40)$$

Equation (40) represents the general solution to our problem which is simply the single-frequency BS result [Eq. (1), Eq. (18) of [2]] summed over the frequency spectrum of the velocity autocorrelation function plus oscillating terms (omitted) that do not contribute as long as $\psi(x) \to 0$ as $x \to \infty$.

### *Example: Particle in circular orbit*

For a particle in an hypothetical circular orbit with orbital frequency $\omega_r \neq \omega_0$ we have

$$\psi(\tau) = v_{xy}^2 \cos \omega_r \tau,$$

$$\psi(\omega) = v_{xy}^2 \delta(\omega - \omega_r), \qquad (41)$$

and substituting in Eq. (40),

$$\delta\omega = -ab \int_{-\infty}^\infty v_{xy}^2 \delta(\omega - \omega_r) \frac{1}{\omega_0^2 - \omega^2} d\omega + \text{(oscillating terms)}$$

$$= -\frac{abv_{xy}^2}{\omega_0^2 - \omega_r^2}, \qquad (42)$$

in agreement with [Eq. (1), Eq. (18) of [2]] and valid for the case when $(\omega_0 - \omega_r) > \omega_{x,y}$.

## III. NUMERICAL CALCULATIONS OF THE FREQUENCY SHIFT

### A. Numerical estimations of the correlation function

The problem of the neutron EDM experiment with a $^{199}$Hg comagnetometer subject to a time-varying $E \times v$ field in combination with a spatially varying magnetic field is described in [2] and in the Introduction. We assume a cylindrical volume with radial field $\vec{B}(r) = a'r\hat{r}$. The electric field is constant everywhere and along the $\hat{z}$ direction. Assuming a constant velocity $v$, in the $x$-$y$ plane, the $E \times v$ field is then fluctuating in direction but of spatially uniform magnitude.

A numerical calculation of the correlation function was performed for the two-dimensional case (UCN or Hg at a fixed $z$, moving only in $x$-$y$ plane). This problem can be parametrized in terms of the time between collisions, $\tau_c = \lambda/v$, where the mean free path between collisions is $\lambda$ and the average velocity is $v$. For the numerical calculations, $v$ is assumed constant. Time can be parametrized in dimensionless units, $\tau/\tau_c$. The correlation function was calculated by statistically choosing a propagation distance for a fixed velocity direction and taking time steps of 0.025, after which a new random velocity direction was chosen. Various degrees of specularity, parametrized by $\Delta\theta$ for the statistical degree of angular change for reflection from the bottle surface, were considered.

Results of a two-dimensional Monte Carlo calculation are shown in Fig. 1. Taking $\lambda = 1$ and fixed, we see the effect of wall collisions as the bottle radius approaches $\lambda$. We see in Fig. 1 that in all cases $R(\tau)$ initially increases linearly. The effect of the wall collisions when $R > \lambda$ is to limit the dis-
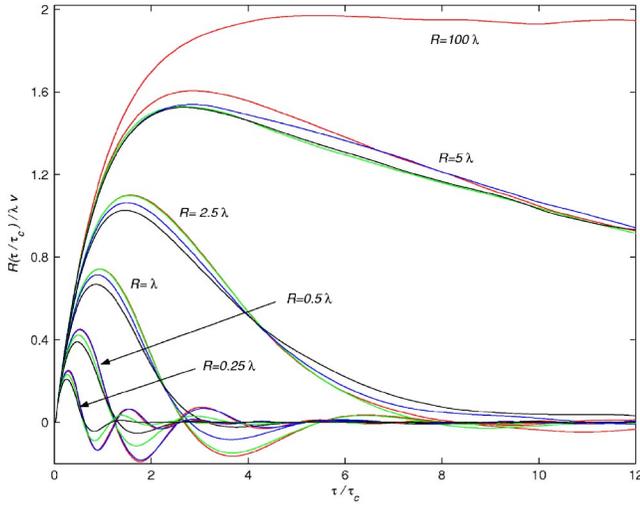
FIG. 1. The position-velocity correlation function $R(\tau) = 2h(\tau)$ as a function of cell radius $R$ parametrized in terms of the mean free path $\lambda$ for different degrees of specularity as parametrized by the angular spread of the final angle compared to the incident angle. The plots for a given $R$ are for angular spreads on reflection of $0°$, $45°$, $90°$, and $180°$, with the latter representing diffuse reflection. Increased angular spread causes the correlation function to decay more rapidly in all cases. For $R \gtrsim 2.5\lambda$, there was practically no effect due to the degree of specularity, as expected.

tance that the random walk can take, and this appears as an exponential decay in $R(\tau)$ at long times. This effect does not depend on the specularity of the wall collisions and is best seen as an effect on the whole ensemble of particles which can be described by classical diffusion theory. In this limit, the correlation function is well described by

$$R(\tau) = (1 - e^{-\tau/\tau_c}) e^{-\tau/T}, \qquad (43)$$

where, from analysis of the plots,

$$T \approx \frac{0.6R^2}{\lambda v}. \qquad (44)$$

In the other limit $R < \lambda$, $R(\tau)$ oscillates with frequency

$$\omega \approx \frac{2\pi v}{5.2R} \qquad (45)$$

and

$$R(\tau) = e^{-\tau/T} \sin \omega\tau, \qquad (46)$$

where $T$ depends on $\Delta\theta$, but is typically of order $2\pi/\omega$.

The frequency shift is determined by Eq. (26) and in the case of large $R$ we find ($\tau_c \ll T$), using Eq. (44),

$$\delta\omega = \frac{abR^2}{T^2\omega_0^2 + 1} = \frac{abR^2}{1 + (0.6R^2\omega_0/v\lambda)^2}. \qquad (47)$$

These results are in good agreement with [2], Fig. 10, for which $4/2\pi \approx 0.634$ replaces the factor 0.6 above and with Eq. (72) below.

Additional insight can be gained by considering the effects of varying $\lambda$ keeping $R$ fixed, as shown in Fig. 2 for
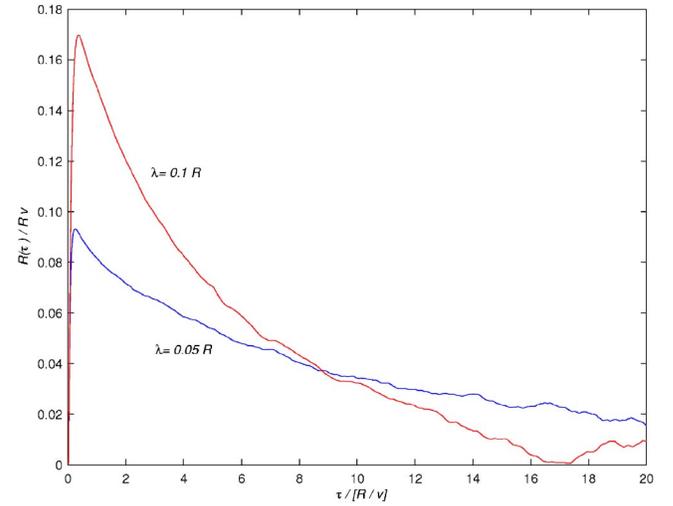


FIG. 2. The position-velocity correlation function when $\lambda$ is very small. This represents the limit for slow diffusion.

very small $\lambda$. In this limit, the horizontal axis is multiplied by $\lambda/R$ to define time proportional to $R/v$. The correlation amplitude function is proportional to $\lambda v$ and the decaying exponential time constant is

$$T \propto \frac{R^2}{\lambda v}. \qquad (48)$$

The time to reach the peak value is

$$\tau_0 \propto \lambda^2/Rv, \qquad (49)$$

which approaches zero as $R \to \infty$.

This limit is further discussed in Sec. V A, and the frequency shift in this case is in general agreement with Fig. 10 of [2].

The curves for large (relative to $R$) $\lambda$ in Fig. 1 show damped oscillations whose damping depends on the angular spread of the wall collisions. This is a manifestation of the resonance behavior discussed in Ref. [2] for the case of perfectly specular wall collisions. Here we see the damping due to nonspecular reflections.

### B. Numerical estimations of the frequency shift for all values of $\omega_0/\omega_r$

Using Eq. (37) and the results of the previous section, the cosine transform of the numerically determined correlation function can be calculated numerically. In order to reduce oscillations due to the finite time window, a Hamming window function was applied to the correlation function and a slight correction due to the frequency dependent gain as imposed by the window function was applied. The results, as a function of mean free path $\lambda$ at fixed radius $R$, for specular and purely diffuse wall reflection, are shown in Fig. 3.

There are a few points worth noting. First, the curves for large $\lambda$ in the specular case are very similar to the Bloch-Siegert result. Second, at small and large frequencies, the results agree with the numerical semianalytically determined results presented above and in [2] and the theoretical analysis
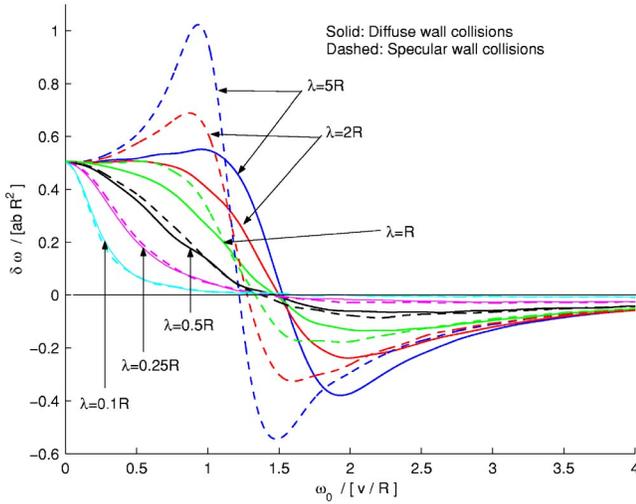
FIG. 3. Results of numerically applying Eq. (37) to numerical calculations of the correlation function, for varying $\lambda$ with $R$ fixed.

below. Third, the behavior at intermediate frequencies is seen to be very interesting: The shift goes to zero for $\omega_0/\omega_r \sim 1$ as it must because the effect changes sign between large and small frequencies.

Furthermore, it can be seen immediately that the effects of wall collision specularity are important when $\omega_0 \approx \omega_r$, in contradiction to the statement in [2] that the degree of specularity does not affect the frequency shift. We discuss this point later in more detail (Sec. IV).

## IV. ANALYTIC RESULTS FOR THE LIMITING CASES OF LARGE AND SMALL FREQUENCIES $(\omega_0/\omega_r \gg 1, \omega_0/\omega_r \ll 1)$

Equation (40) represents the formal solution of the problem in all cases of interest here. Thus the frequency shift is determined entirely by the velocity autocorrelation function of the particles undergoing magnetic resonance. This function has been the subject of intense experimental and theoretical study [9–12]. In our case, involving macroscopic distances and times, it suffices to treat the motion classically. For relatively short times, if the particles undergo collisions which are distributed according to a Poisson distribution with average time between collisions given by $\tau_c$, the velocity correlation function is well known to be given by

$$\psi(t) = \langle v^2 \rangle e^{-t/\tau_c}. \tag{50}$$

This form is known to be valid for relatively short times. According to Eq. (37) the frequency shift depends on the Fourier transform of the integral of the velocity correlation function evaluated at $\omega_0$. So the short-time behavior of $\psi(t)$ determines the high-frequency behavior of $\psi(\omega)$, and the result using this form is expected be valid in the case of large $\omega_0$—i.e., $\omega_0 \gg \omega_r$.

For longer times the velocity correlation function is well described by classical diffusion theory. Thus the long-time behavior will determine the low-frequency region of the velocity spectrum and the result will apply to the case $\omega_0$

$\ll \omega_r$. In this region the result will depend on the size of the containing vessel as the dynamics of the diffusion process are influenced by the boundary conditions.

### A. Short correlation times $(\omega_r \ll \omega_0)$

Using Eq. (50) we have

$$\psi(\omega) = \frac{1}{\pi} \langle v^2 \rangle \int_0^\infty \cos \omega t e^{-t/\tau} dt = \frac{1}{\pi} \langle v^2 \rangle \frac{1}{\tau(\omega^2 + 1/\tau^2)}, \tag{51}$$

so that, according to Eq. (40),

$$\delta\omega = -ab \int_{-\infty}^\infty \frac{\psi(\omega)}{(\omega_0^2 - \omega^2)} d\omega \tag{52}$$

$$= ab \frac{1}{\pi} \frac{\langle v^2 \rangle}{\tau} \int_{-\infty}^\infty \frac{1}{(\omega^2 + 1/\tau^2)(\omega^2 - \omega_0^2)} d\omega \tag{53}$$

$$= -ab \frac{\langle v^2 \rangle}{\omega_0^2} \frac{1}{(1 + 1/\omega_0^2 \tau^2)}. \tag{54}$$

This is in substantial agreement with the expression given in the caption of Fig. 12 of [2] when it is taken with Eq. (19) or (3) of [2] applicable to the case when $\omega_r \ll \omega_0$. It is quite likely that the small discrepancy ($\sim 10\%$) in the 50% suppression point is due to the process of averaging over the velocity distribution shown in Fig. 12 of [2].

### B. Diffusion theory calculation of the long-time behavior of the velocity correlation function: Frequency shifts for $(\omega_r \gg \omega_0)$

Whereas the previous case applies to UCN this case would apply to atoms used as a comagnetometer and is more relevant experimentally as it results in larger shifts [2] and in some cases [13] the collision rate can be simply adjusted by changing the experimental conditions.

In the following we review the solution of the diffusion equation in cylindrical geometry, obtain the velocity autocorrelation function from the solution, and calculate the frequency shift. In the limit of a small collision rate the result agrees with the known results for $(\omega_r \gg \omega_0)$ and the effect of the collisions agrees with that found from numerical simulations (Fig. 10 of [2]).

#### 1. Green's function for the diffusion equation in cylindrical geometry

In this section we attempt to understand the effects of the vessel boundary on the velocity autocorrelation function, observed in the numerical simulations (Sec. III A), by applying classical diffusion theory to the problem. Diffusion theory is expected to be valid for long times so that we expect the results to be valid for small $\omega_0$—i.e., $\omega_0 \ll \omega_r$:

$$D\nabla^2 \rho - \frac{\partial \rho}{\partial t} = 0,$$

$$\rho = u_k(r)e^{-Dk^2t},$$

$$\nabla^2 u + k^2 u = 0. \qquad (55)$$

We consider a two-dimensional problem; that is, we neglect any $z$ dependence ($k_z = 0$). For the cases considered in [2] where the height of the bottle is much smaller than the radius higher-$z$ modes will decay relatively quickly.

The boundary condition is $j(R) = -D\,\partial\rho/\partial r = 0$, so the eigenfunctions satisfying the boundary conditions are

$$u_{m,n} = N_{m,n}J_m(k_{m,n}r)e^{im\theta},$$

$$k_{m,n}R = x_{m,n}[n\text{th zero of } dJ_m(z)/dz],$$

where the normalization constant (which depends on the boundary conditions) is ([14], p 322)

$$N_{m,n} = \frac{1}{\sqrt{2\pi}J_m(k_{m,n}R)}\sqrt{\frac{2k_{m,n}^2}{(k_{m,n}R)^2 - m^2}}. \qquad (56)$$

The Greens' function satisfying the boundary conditions is [15]

$$G(r,r',t) = \sum_{m,n}(N_{m,n})^2 J_m(k_{m,n}r)J_m(k_{m,n}r')e^{im(\theta-\theta')}e^{-Dk_{m,n}^2t}. \qquad (57)$$

This is the probability of finding a particle at $\vec{r}$ at time $t$, given that the particle was at $\vec{r}'$ at time $t=0$. The spectrum of the velocity correlation function is related to $S(\vec{q},\omega)$ which in turn is the average over the system of the Fourier transform of this probability with respect to $\rho = (r-r')$. We use the cosine transform because we want the cosine transform of the velocity correlation function (38) $\psi(\omega)$:

$$S(q,\omega) = \frac{1}{\pi}\left\langle \int d^2\rho\, e^{i\vec{q}\cdot\vec{\rho}}\int_0^\infty dt\cos\omega t\, G(r,r',t)\right\rangle \qquad (58)$$

$$= \frac{1}{\pi}\int\int \frac{d^2r'}{\pi R^2}d^2\rho\, e^{i\vec{q}\cdot\vec{\rho}}\int_0^\infty dt\cos\omega t\, G(r,r',t) \qquad (59)$$

$$= \frac{1}{\pi^2 R^2}\sum_{m,n}(N_{m,n})^2\int d^2r\, e^{i\vec{q}\cdot\vec{r}}J_m(k_{m,n}r)e^{im\theta} \qquad (60)$$

$$\int d^2r'\, e^{-i\vec{q}\cdot\vec{r}'}J_m(k_{m,n}r')e^{-im\theta'}\frac{Dk_{m,n}^2}{\omega^2 + (Dk_{m,n}^2)^2}. \qquad (61)$$

Now we can evaluate the integrals using

$$J_m(x) = \frac{(-i)^m}{2\pi}\int_0^{2\pi}e^{i(x\cos\theta + m\theta)}d\theta \qquad (62)$$

and Bessel function identities

$$\int d^2r\, e^{i\vec{q}\cdot\vec{r}}J_m(k_{m,n}r)e^{im\theta} = \frac{2\pi(i)^{\pm m}}{(q^2 - k_{m,n}^2)}\frac{qR}{2}J_m(k_{m,n}R)[J_{m-1}(qR) - J_{m+1}(qR)]. \qquad (63)$$

Thus,

$$S(q,\omega) = \frac{2}{\pi^3 R^2}\sum_{m,n}\frac{k_{m,n}^2}{(k_{m,n}R)^2 - m^2}\left(\frac{2\pi}{(q^2 - k_{m,n}^2)}\frac{qR}{2}[J_{m-1}(qR) - J_{m+1}(qR)]\right)^2\frac{Dk_{m,n}^2}{\omega^2 + (Dk_{m,n}^2)^2}. \qquad (64)$$

### 2. Velocity autocorrelation function

The velocity autocorrelation function

$$\psi(\tau) = \langle\vec{v}(0)\cdot\vec{v}(\tau)\rangle \qquad (65)$$

has a Fourier transform given by [16]

$$\psi(\omega) = \lim_{q\to 0}2\left(\frac{\omega}{q}\right)^2 S(q,\omega), \qquad (66)$$

so that the only terms in Eq. (64) which contribute are those containing $J_0(qR)$, since $\lim_{x\to 0}J_n(x) \sim (x)^n$, $J_0(0) = 1$. Thus we only need to keep terms with $m = \pm 1$ in Eq. (64) and we find

$$\lim_{q\to 0}S(q,\omega) = \frac{2q^2}{\pi[(k_{1,n}R)^2 - 1]}\frac{D}{\omega^2 + (Dk_{1,n}^2)^2}. \qquad (67)$$

Then

$$\psi(\omega) = \frac{1}{\pi}\sum_n\frac{4}{x_{1,n}^2 - 1}\frac{D\omega^2}{\omega^2 + (Dk_{1,n}^2)^2}. \qquad (68)$$

### 3. Frequency shift in the diffusion approximation (cylindrical geometry)

According to Eq. (40),

$$\delta\omega = -ab\int_{-\infty}^{\infty}\psi(\omega)\frac{1}{\omega_0^2 - \omega^2}d\omega \qquad (69)$$

$$= abR^2\sum_n\frac{4}{x_{1,n}^2 - 1}\frac{1}{x_{1,n}^2[(\omega_0 R^2/Dx_{1,n}^2)^2 + 1]}. \qquad (70)$$

The result (70) is dominated by the first mode $x_{1,1} = 1.84$. Figure 4 shows the first term in comparison to the sum of the first five terms. For convenience we list the zeros of $J_1'(x)$: $x_{1,2} = 5.33$, $x_{1,3} = 8.54$, $x_{1,4} = 11.7$. Since we are dealing with a two-dimensional problem, we put

$$D = v^2\tau/2 \qquad (71)$$

(instead of $\pi v^2/3$ for three dimensions) in order to facilitate the comparison with the numerical simulations [2] and obtain for the condition that the frequency shift be reduced to 50% of its value in the absence of collisions,

$$\eta = \frac{\omega_0 R^2}{Dx_{1,n}^2} = \frac{2\omega_0 R^2}{v^2\tau x_{1,n}^2} = 0.59\frac{\omega_0 R^2}{v^2\tau} = 1, \qquad (72)$$

the numerical factor of which is to be compared with $2/\pi = 0.634$ obtained in [2], Fig. 10, by fitting simulated results, and our numerical result of 0.6 presented in Sec. III A. The magnitude $abR^2/2$ of Eq. (70) in the absence of collisions is
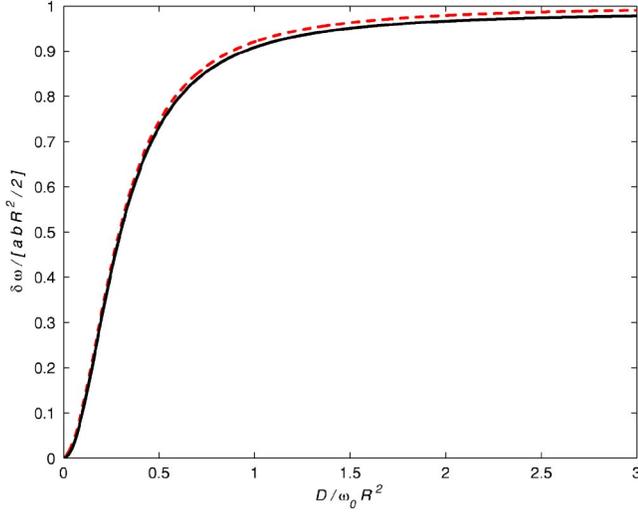
FIG. 4. Plot of Eq. (68). Solid line: first term. Dashed line: sum of first five terms.

just that expected from the Bloch-Siegert treatment in the case $\omega_r \gg \omega_0$ [Eq. (3), Eq. (21) of [2]], averaged over the different trajectories as discussed in [2] after Eq. (22).

### 4. Frequency shift in the diffusion approximation (rectangular geometry)

For the rectangular case the normalized eigenfunctions are

$$u_{m,n}(x,y) = \sqrt{\frac{2}{L_x}} \cos \frac{m\pi}{L_x} x \sqrt{\frac{2}{L_y}} \cos \frac{m\pi}{L_y} y, \qquad (73)$$

which satisfy the reflection boundary conditions at $x=0$, $L_x$ and $y=0$, $L_y$. For $n$ or $m=0$ the corresponding eigenfunctions are

$$u_0 = \frac{1}{\sqrt{L_{x,y}}}, \qquad (74)$$

so that the Green's function is

$$G(x,x',y,y',t) = \sum_{m,n=0}^{\infty} \left[ \frac{1}{L_x} + \frac{2}{L_x} \cos k_m x \cos k_m x' e^{-Dk_m^2 t} \right]$$
$$\times \left[ \frac{1}{L_y} + \frac{2}{L_y} \cos k_n x \cos k_n x' e^{-Dk_n^2 t} \right], \quad (75)$$

with $k_{m,n}=(m,n)\pi/L_{x,y}$. To calculate $\lim_{q\to 0} S(q,\omega)$ we need integrals of the form

$$\lim_{q\to 0} \int_0^L e^{iq_x x} \cos k_m x \, dx = \frac{q_x}{q_x^2 - k_m^2} \begin{Bmatrix} q_x L_x, & m=2,4,6,\dots \\ -2/i, & m=1,3,5,\dots \end{Bmatrix} \qquad (76)$$

$$= \{L_x, \quad m=0\}. \qquad (77)$$

Since each of these will appear squared because of the contribution from the $x$, $x'$ integrals, we can only take the odd values of $m$. The even numbers will yield a higher power of

$q$ which will vanish in the limit. Given this, if we take $m=1,3,5$, we must take $n=0$ and vice versa. We calculate, using Eq. (76),

$$\lim_{q\to 0} \left[ S(q,\omega) = \int dx \int \frac{dx'}{L_x} \int dy \int \frac{dy'}{L_y} e^{i\vec{q}\cdot(\vec{x}-\vec{x}')} \frac{1}{\pi} \right.$$
$$\left. \times \int_0^{\infty} dt \cos \omega t \, G(\vec{x},\vec{x}',t) \right] \qquad (78)$$

$$= q^2 \frac{8}{2\pi} \left( \sum_{m=1,3,5,\dots} \frac{1}{k_m^2 (m\pi)^2} \frac{Dk_m^2}{\omega^2 + (Dk_m^2)^2} \right.$$
$$\left. + \sum_{n=1,3,5,\dots} \frac{1}{k_n^2 (n\pi)^2} \frac{Dk_n^2}{\omega^2 + (Dk_n^2)^2} \right), \qquad (79)$$

where we used $\langle q_x^2 \rangle = \langle q_y^2 \rangle = q^2/2$. Then,

$$\psi(\omega) = \frac{8\omega^2}{\pi} \left( \sum_{m=1,3,5,\dots} \frac{1}{k_m^2 (m\pi)^2} \frac{Dk_m^2}{\omega^2 + (Dk_m^2)^2} \right.$$
$$\left. + \sum_{n=1,3,5,\dots} \frac{1}{k_n^2 (n\pi)^2} \frac{Dk_n^2}{\omega^2 + (Dk_n^2)^2} \right) \qquad (80)$$

and [using Eq. (40)]

$$\delta\omega = -ab \int_{-\infty}^{\infty} \psi(\omega) \frac{1}{\omega_0^2 - \omega^2} d\omega \qquad (81)$$

$$= 8ab \left( \sum_{m=1,3,5,\dots} \frac{L_x^2}{(m\pi)^4} \frac{1}{(\omega_0 L_x^2/D(m\pi)^2)^2 + 1} \right.$$
$$\left. + \sum_{n=1,3,5,\dots} \frac{L_y^2}{(n\pi)^4} \frac{1}{(\omega_0 L_y^2/D(n\pi)^2)^2 + 1} \right). \qquad (82)$$

We thus see that in a rectangular box $L_x \neq L_y$ it is the longer side which dominates the behavior.

### C. Application: ³He comagnetometer

In Ref. [13] the use of ³He as a comagnetometer for a UCN neutron EDM experiment is discussed. This system is rather unique in that an effective background gas (phonons) can be introduced which affects the ³He significantly while having no substantial interaction with the UCN for temperatures below 0.5 K. Because the ³He and neutron magnetic moments are equal to within 10%, it is possible to control this systematic by varying the size of the effect for ³He by changing the diffusion rate of the ³He atoms.

The UCN upscattering lifetime varies as $100T^{-7}$ s for $T < 0.7$ K, while the coefficient of diffusion for ³He in a superfluid helium bath varies as $D \approx 1.6T^{-7}$ cm²/s [19].

In connection with Eq. (72) this yields $\eta=1$ when the superfluid helium temperature is $T \approx 0.25$ K $(R=25$ cm), which determines the temperature scale where the effect can be varied, and is within the design range of operating temperature for the planned experiment, compatible with a UCN upscattering lifetime in excess of 1000 s.

## V. DISCUSSION

One of the surprising, but unexplained, results of [2] was that according to their numerical simulations, wall collisions had no influence on the magnitude of the frequency shifts while gas collisions could eliminate the frequency shifts completely if their rate is high enough. This was apparently only studied in the limits of large and small $\omega_0/\omega_r$. We now know that this does not apply to intermediate frequencies—e.g, when $\omega_0 \sim \omega_r$. In Fig. 3 we see that wall collisions have a serious influence at intermediate frequencies when $\lambda \geq R$. Also, from Fig. 3, we see that the curves for diffuse wall reflections are very similar to the specular curves for $\lambda < R/2$. This implies that there is no essential difference between wall and gas collisions. We now show that the reason the wall collisions have no effect at the limiting frequencies, contrary to the case at intermediate frequencies, is that the wall collisions are never fast enough to influence the systematic (proportional to $\vec{E}$) frequency shifts in the limits of large and small $\omega_0$.

For a particles in a cylindrical vessel following a trajectory along a chord subtending an angle $2\alpha$, the time between collisions is

$$\tau_c = \frac{2R}{v} \sin \alpha \qquad (83)$$

and the effective field rotation frequency is given by

$$\omega_r = 2\alpha/\tau_c = \frac{\alpha v}{R \sin \alpha}. \qquad (84)$$

Considering first the case when $\omega_r \gg \omega_0$ [Eq. (70), Fig. 10 of [2]], the systematic frequency shift was found to be suppressed by the factor $\eta$:

$$\eta = \frac{1}{1 + \beta^2},$$

$$\beta = \frac{2R^2 \omega_0}{\pi v^2 \tau_c}.$$

For significant suppression we need $\beta \gtrsim 1$,

$$\frac{2R^2 \omega_0}{\pi v^2 \tau_c} = \frac{R \omega_0}{\pi v \sin \alpha} \gtrsim 1,$$

$$\sin \alpha \lesssim \frac{R \omega_0}{\pi v} = \frac{25 \times 2 \times 7}{10^4} \sim \frac{1}{30}, \qquad (85)$$

for representative conditions in [2], Fig. 10 ($R=25, B_0 = 1\ \mu\text{T}, v = 10^4\ \text{cm/s}$).

The probability of a given value of $\alpha$ is given in Eq. (B1) of [2] as

$$P(\alpha)d\alpha = \frac{4}{\pi} \sin^2 \alpha\, d\alpha,$$

$$P(\alpha \leq \varepsilon) \sim \varepsilon^3, \qquad (86)$$

so that the wall collisions would only be expected to be effective for a vanishingly small fraction of the trajectories.

Turning now to the case $\omega_r \ll \omega_0$ [Eq. (54), Fig. 12 of [2]] we have, as the condition that the suppression be effective,

$$\beta = \frac{1}{\omega_0 \tau_c} \geq 1,$$

$$\frac{1}{\omega_0} \gtrsim \frac{2R}{v} \sin \alpha,$$

$$\sin \alpha \leq \frac{v}{2R\omega_0} = \frac{200}{2 \times 25 \times 200} = \frac{1}{50},$$

for conditions typical of [2], Fig. 12 ($v=200\ \text{cm/s}, B_0 = 1\ \mu\text{T}$).

Thus the wall collisions rate is never high enough to significantly affect the magnitude of the frequency shift at the limits. The wall collisions do, however, broaden and shift the resonances discussed in [2]

## VI. CONCLUSION

We have developed a general technique of analyzing the systematic effects due to a combination of an electric field and magnetic gradients as encountered in EDM experiments that employ gasses of stored particles. Use of the correlation technique, either by numerical calculations for complicated geometries or by the velocity correlation function for simpler geometries, provides a simplified approach to the problem compared to numerical integration of the Bloch equations. Our analysis has added insight to this new systematic effect and provides a means of rapidly assessing the effects of various geometries and angular distributions for wall and gas collisions.

## APPENDIX: MATRIX ALGEBRA OF SPHERICAL PAULI MATRICES

The following relationships among the Pauli matrices have been employed in the calculation in Sec. II A:

$$2\sigma_\pm = \sigma_x \pm i\sigma_y, \qquad (A1)$$

$$\sigma_\pm \sigma_z = \mp\, \sigma_\pm, \quad \sigma_z \sigma_\pm = \sigma_\pm, \qquad (A2)$$

$$\sigma_\pm \sigma_\mp = \frac{1}{2} \pm \frac{1}{2}\sigma_z, \qquad (A3)$$

$$\sigma_z \sigma_z = 1, \quad \sigma_\pm \sigma_\pm = 0. \qquad (A4)$$

[1] Eugene D. Commins, Am. J. Phys. **59**, 1077 (1991).

[2] J. M. Pendlebury *et al.*, Phys. Rev. A **70**, 032102 (2004).

[3] N. F. Ramsey, Phys. Rev. **100**, 1191 (1955).

[4] D. D. McGregor, Phys. Rev. A **41**, 2631 (1990).

[5] G. D. Cates, S. R. Schaefer, and W. Happer, Phys. Rev. A **37**, 2877 (1988).

[6] G. D. Cates *et al.*, Phys. Rev. A **38**, 5092 (1988).

[7] S. K. Lamoreaux, Phys. Rev. A **53**, R3705 (1996).

[8] A. Abragam, *Principles of Nuclear Magnetism* (Clarendon Press, Oxford, 1961).

[9] G. L. Squires, *Introduction to the Theory of Thermal Neutron Scattering* (Cambridge University Press, Cambridge, England, 1978).

[10] J.-P. Boon and S. Yip, *Molecular Hydrodynamics* (McGraw-Hill, New York, 1980).

[11] Peter A. Egelstaff, *An Introduction to the Liquid State* (Academic Press, New York, 1967).

[12] Stephen W. Lovesey, *Theory of Neutron Scattering from Condensed Matter* (Clarendon Press, Oxford, 1984).

[13] R. Golub and S. K Lamoreaux, Phys. Rep. **237**, 1 (1994).

[14] A. Sommerfeld, *Partial Differential Equations* (Academic Press, New York, 1967).

[15] Philip M. Morse and Herman Feshbach, *Methods of Theoretical Physics* (McGraw-Hill, New York, 1953), Chap. 7.

[16] This theorem, apparently based on work of de Gennes [17] was first stated by Egelstaff [18] and has been cited by many authors with slightly different numerical constants. The most complete proofs are given in [9] and [10]. The form we have used is appropriate for our two-dimensional problem. A more detailed discussion of this and a new derivation of the theorem are given in an extended version of the present work to be found at www.ArXiv.org (e-print nucl-ex/0407005).

[17] P. G. de Gennes, Physica (Amsterdam) **25**, 825 (1959).

[18] P. A. Egelstaff, in *Proceedings of the Symposium on Inelastic Scattering of Neutrons in Solids and Liquids* (IAEA, Vienna, 1961), p. 25.

[19] S. K. Lamoreaux *et al.*, Europhys. Lett. **58**, 718 (2002).